MULTI-PHYSICAL SIMULATIONS OF DENSE GRANULAR FLOWS BY MESH-FREE METHOD

A Thesis

Submitted to the Faculty of Graduate Studies and Research

In Partial Fulfillment of the Requirements

For the Degree of

Master of Science

in

Environmental Systems Engineering

University of Regina

By

Luoyilang Ke

Regina, Saskatchewan

October, 2017

UNIVERSITY OF REGINA

FACULTY OF GRADUATE STUDIES AND RESEARCH

SUPERVISORY AND EXAMINING COMMITTEE

Luoyilang Ke, candidate for the degree of Master of Applied Science in Environmental Systems Engineering**,** has presented a thesis titled, ***Multi-Physical Simulations of Dense Granular Flows by Mesh-Free Method,*** in an oral examination held on September 1, 2017. The following committee members have found the thesis acceptable in form and content, and that the candidate demonstrated satisfactory knowledge of the subject material.

External Examiner:	Dr. Kei Lo, Sask Water Security Agency
Supervisor:	Dr. Yee-Chung Jin, Environmental Systems Engineering
Committee Member:	Dr. Peng Wu, Environmental Systems Engineering
Committee Member:	Dr. Babak Mehran, Environmental Systems Engineering
Chair of Defense:	Dr. Irfan Al-Anbagi, Electronic Systems Engineering

Abstract

Recently, applying mesh free method coupled with a constitutive rheology has achieved success in modeling dynamics in dry granular flows. However, research on comprehensive validation on the coupled model in different aspects, such as pressure, velocity, shear stress, surface, friction factor and different geometries is limited. In this study, three different cases, including gravity driven flow, 2D column collapse and granular dam-break are simulated to validate the coupled model of MPS method with $\mu(I)$ rheology model, by comparing the simulated results with analytical solutions and experimental results. In the simulations, flow characteristics are successfully captured in dry granular flows in different flow scenarios. In gravity driven flow, MPS reproduces a steady uniform zone in which good agreements have been achieved in terms of pressure, shear stress, friction factor and velocity distribution comparing numerical results with analytical solutions. In 2D column collapse and granular dam-break flow, the MPS has good performance in capturing dynamic features observed and measured in labs. After validation of the coupled model, numerical results pressure, tangential stress and friction factor are analyzed and discussed. It is found that the coupled model can be used to distinguish flow regimes in granular flows according to calculated pressure, stress, and friction factor. In numerical results, non-linear distributions with an obvious change on the free surface for the pressure and stress are observed. This study lays solid examples to show that the MPS method coupled with $\mu(I)$ rheology model is a useful numerical tool to reflect flow characteristics in granular flows.

Keywords: MPS, granular flow, rheology model, stress, friction factor

Acknowledgement

I would like to give my great thanks to those who support and helped me to finish my master degree. Without their experienced suggestion and enthusiastic encouragement, many problems and difficulties could not be solved. I also would like to show my deepest appreciation and respect to my supervisor Prof. Yee-chung Jin, DR. Tibing Xu and my parents.

First, I want to say thanks to my supervisor Prof. Yee-chung Jin. For my study, his solid and extensive research experience enlightened me to have more creative ideas and avoid mistakes. Meanwhile, he was very patient to cultivate me on the attitude of research, which made me realizing that the academic research was a serious work. Financially, he provided scholarship to support me, which makes me focusing on study without pressure from living.

Second, I would like to thank DR. Tibing Xu. With his strong theoretical knowledge of MPS method and granular flow, he helped me to quickly understand the rheology of the model and granular flow, and his experience of research helped me a lot to complete my thesis.

Finally, I want to say thanks to my parents. They mentally and financially supported me to study abroad, so I had a chance to finish my master degree in Canada.

Table of Content

Table of Figures

CHAPTER ONE: Introduction and objective

1.1 Objective of researching granular flow and introduction of granular flow

Granular flows naturally occur resulting in risks to human safety. The understanding of the fluid mechanics and dynamics of granular flow, such as rock fall, debris flow, ice avalanche, and transferring agricultural or pharmaceutical products has been an important subject in geotechnical engineering. Figure 1 shows the large scales of rock fall and ice avalanche. Those destructive phenomena are possible potential rise to threat human's life and damage facilities. For example, in Liu, N. (2015), the earthquake in Lu Dian located at the southwestern of china caused the huge deposition of granular materials moving 1000 meters to a river, and the river was blocked by granular materials. In Figure 1, the granular flow also appears in the agricultural industry, which indicate that the rheology of granular flow is properly utilized to improve efficiency of industrial activities. Therefore, it is important and worth to research granular flows, which can help prevent disaster or effectively using resources. Flow behavior and characteristics are difficult to predict due to the granular texture, size, shape, heterogeneity and density of the granular materials. Research on flow behaviors caused by these materials is very important and necessary to take precautionary measures to minimize the environmental and social impacts caused by such landslides, or improve industrial efficiency in transfer and storing the materials

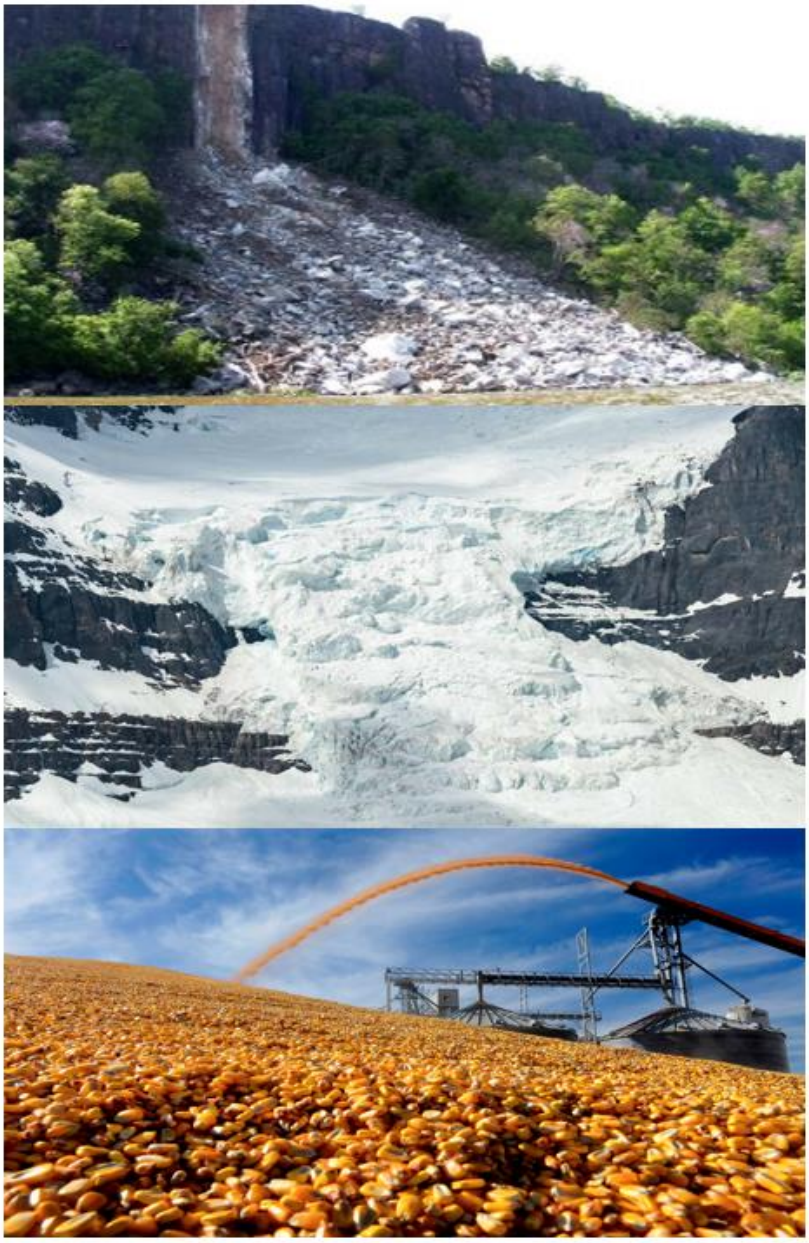

Figure 1 Granular flow in natural environment

Sited from:

http://blogs.ei.columbia.edu/2012/05/16/rock-fall-shakes-new-jersey-palisades/

http://roadslesstraveled.us/jasper-national-park-columbia-icefields-athabasca-falls/

http://leyok.h.media.illinois.edu/jour425wp/?tag=agriculture

Under different environments, different factors could affect granular flow. For example, the wet granular flow is affected by cohesion of water, but, the cohesion of water has no effect in dry granular flow. In this study, only dry granular material is considered. Although the flow of dry sand seems having a simple flow behavior, lots of research shown that the dry granular flow is still a complicated flow (Andreotti 2007, Brodu et al 2013, Cruz et al 2005). The behavior of granular material can be identified as different states under different circumstances (Jaeger et al 1996, de Gennes 1999 and Takahashi 2014). Granular flow can occur in solid-like and liquid-like states (Vescovi et al. 2016), Under sufficiently packed condition, a fix or stable structure is formed by granular grains, which limits the granular movement, resulting in behave like solid as solid-like state. When the behavior is dominated by macroscopic deformation and inertial timescales, the material transforms into a fluid-like state. Previous studies (Forterre and Pouliquen 2008, Xu and Jin 2016, Xu, et al. 2016) showed that granular flow is able to be categorized into three regimes. In the first regime called the quasi-static regime or static regime, granular grains have low velocity, which exhibit creeping flow. The second regime is the dense regime or transitional regime, where grains are in close contact with each other; however, inertia still plays an important role to the material (Xu and Jin 2016). The third regime is defined as the gaseous regime, in which granular grains have very high velocity causing a loss of network structure between grains. In most cases, the granular flows in the fluid-like state can transition from the gaseous regime to the dense regime or to quasi-static regime due to energy dissipation, or from the quasi-static regime to gas regime. The dynamic transition between the various regimes creates challenges in describing the general theory of granular flows.

1.2 Objective of applying MPS coupled with $\mu(I)$ rheology model

To describe the dynamic granular flow state, the soil plasticity models are used in the quasi-static regime while the kinetic theory is applied for the gaseous regime. To represent macropore deformation and the inertial effect in the dense regime, constitutive laws have been developed to describe the flow behavior. There are many models proposed for dense granular flows, but most of them are only applicable to specific scenarios (Sela and Goldhirsch 1998 , Garzó and Dufty 1999). A constitutive law, such as the $\mu(I)$ rheology model, has been developed by taking into account of the wide range of configurations in granular flows (Jop et al. 2006, Cruz et al. 2005). Previous studies have successfully utilized the rheology model to describe dense granular flow (Chauchat and Médale 2014, Capart et al. 2015, MiDi (2004), Lagrée et al. 2011). In the rheology model, the yield condition separating quasi-static and the dense regime is incorporated into the model to allow for different states of the granular flow with multiple regimes. The advantage of applying the theology model is that it can reliably represent and calculate dynamics of granular flow in dense regime. So, the $\mu(I)$ rheology model is applied to all cases in my study.

With the diverse ability of $\mu(I)$ rheology model to simulate and accurately represent granular flow and interfacial changes in granular materials, the coupling of a numerical method such as the mesh-free method shows promise. Traditional mesh-based numerical methods have been developed and extensively applied for computational fluid dynamics such as finite difference, finite element, finite volume and other mesh based methods. In

finite difference method and finite element method, the special technique, such as Volume of Fluid (VOF), is needed to simulate deformation of fluid and interface (Hirt and Nichols 1981). However, the advancement and development of mesh-free methods including Smooth Particle Hydrodynamics (SPH) (Ikari and Gotoh 2016)) and Moving Particle Semi-implicit method (MPS) (Koshizuka and Oka 1996) provides flexibility and an innovative approach to address and model deformation flow processes. The advantage of the MPS method is that the movable and deformable surface can be automatically traced in flows and have shown to be of promise in accurately simulating hydraulic jumps, water dam-break, water jet and non-deformable submarine landslide (Koshizuka and Oka 1996, Xu and Jin 2016, Jin et al. 2016). With the character of rheology model and MPS method, the coupling of the rheology model and MPS method has been previously applied to simulate granular flow characteristics (Xu and Jin 2016). However, limited work has been completed in comprehensively validating and analysis of the coupled model under different aspects and configurations in simulating deformational flow conditions under critical state conditions. As mentioned previously, the advantage of MPS method is that the deformable free surface can be easily traced and simulated. In most situation, granular flow is a deformable free surface flow. Many researches have successfully achieved good result in simulating free surface flow under deformable condition, such as the water dam break (Koshizuka and Oka 1996), and deformable landslide (Fu and Jin 2015). The deformable landslide under water modeled by Fu and Jin (2015) is a successful approach to simulate sediment flow using Herschel-Bulky rheology model coupled with MPS method. the simulation of deformable solid material proves that MPS is a possible and reliable choice to simulate granular flow when accurate rheology model is chosen. The $\mu(I)$ rheology

model is one of the proper rheology model to describe granular flow in dense regime and identify different flow regimes in granular flow. The $\mu(I)$ described shear stress like eq. (18). Since the shear stress is pressure and velocity dependent value, the MPS provide the movement and pressure at prediction step calculated by eq. (12) to calculate shear stress. Not only, the parameters captured by MPS satisfy calculation of shear stress $\mu(I)$ rheology model. Both MPS and $\mu(I)$ rheology model share the assumption of incompressibility. Therefore, the MPS method coupled with $\mu(I)$ rheology model is a very good combination to simulate granular flow.

Few researches have simulated granular flow by applying particle method coupled with rheology model. For example, Ikari and Gotoh (2016) proposed SPH particle method coupled with Hooke's law to simulate granular flow, but only surface distribution and velocity is discussed in their study. Chambon et al. (2011) presented SPH particle method coupled with $\mu(I)$ rheology model to simulate granular flow, but one specific scenario is presented to compare with analytical solution. In natural environment or industrial application, not only the pressure, shear stress, friction factor, velocity and flow regimes are important factor in granular flow, but also the geometry varies in different situation. Therefore, in this study, it is necessary to show the validation of different parameters and flow on different geometries, which proves the MPS coupled with $\mu(I)$ rheology model is able to describe different scenario of granular flow existed in natural environment or industrial application.

The aim of this study was to assess the flexibility and robustness of the coupled rheology model in the MPS method in simulating deformational flow dynamics under different flow conditions and environments. To deliver this aim, the objective is to determine the pressure, velocity distribution, friction factor and the shear stress under granular flow conditions in order to validate the robustness and flexibility of the rheology model and MPS approach. Quantifying the variations in the performance of the coupled model was completed under three (3) different configurations: (i) granular flow on an inclined plane; (ii) instantaneous collapse of a granular material in a column; and (iii) dam-break scenario. The investigation will provide more multi-physical insights in the granular flows, which could be potentially extended to real geotechnical engineering projects such as landslide and debris flow.

CHAPTER TWO: MPS method with rheology model

2.1. MPS method

Granular materials in the dense regime are considered as liquid flow. The granular flow is represented in the model by using a mesh free method in the Lagrangian framework. This method has been developed for open channel flow in different geometries (Fu and Jin 2013, Shakibaeinia and Jin 2011) and simulated granular flow as a continuum approach (Xu and Jin 2016). The governing equations are expressed as:

$$\frac{\mathrm{D}\rho}{\mathrm{D}t} = 0 \tag{1}$$

$$\rho \frac{\mathrm{D}\boldsymbol{u}}{\mathrm{D}t} = -\nabla p + \nabla \cdot \boldsymbol{\tau} + \rho \boldsymbol{g} \tag{2}$$

where ρ is the bulk density, $\boldsymbol{u}$ is velocity, p is pressure, $\boldsymbol{\tau}$ is stress tensor and $\boldsymbol{g}$ is the external force such as gravity, ∇ called del is a vector differential operator. For example, the divergence of a vector field can be expressed as:

$$\nabla \cdot \vec{v} = \partial v_x / \partial x + \partial v_y / \partial y + \partial v_z / \partial z$$

The time-splitting scheme to solve the governing equations is the predictor-and-corrector. The predictor calculates intermediate location and velocity, which can be used to calculate the particle number density $\langle n \rangle^*$ and pressure field. The equations in the predictor are:

$$\boldsymbol{u}^{*} = \boldsymbol{u}^{k} + \frac{\nabla \cdot \boldsymbol{\tau}}{\rho} \Delta t + \boldsymbol{g} \Delta t \tag{3}$$

$$\boldsymbol{r}^{*} = \boldsymbol{r}^{k} + \boldsymbol{u}^{*} \Delta t \tag{4}$$

where $\boldsymbol{u}^{*}$ is the intermediate velocity, $\boldsymbol{u}^{k}$ is the velocity at previous time step, Δt is the time step, $\boldsymbol{r}^{*}$ is the intermediate particle location, $\boldsymbol{r}^{k}$ is the particle location at previous time step.

According to results in the predictor, equations in the corrector calculate the new velocity and particle location fields:

$$\boldsymbol{u}^{k+1} = \boldsymbol{u}^{*} - \frac{\nabla p}{\rho} \Delta t \tag{5}$$

$$\boldsymbol{r}^{k+1} = \boldsymbol{r}^{k} + \boldsymbol{u}^{k+1} \Delta t \tag{6}$$

where $\boldsymbol{u}^{k+1}$ is the new velocity, and $\boldsymbol{r}^{k+1}$ is the updated position for particles.

In MPS, a weighting function (kernel function) will be applied to weight particle interaction in searching radius. In figure 2, the movement of all particles in searching radius r_e affect the movement of target particle, but the extent of effect is different based on distance between target particle and surrounding particles in searching radius. The weighting function (kernel function) is to determine the extent of effect for different surrounding particles. In this study, the kernel function is:

$$w\left(r_{ij}, r_e\right)=\begin{cases}\left(1-\dfrac{r_{ij}}{r_e}\right)^3 & r_{ij} \le r_e \\ 0 & r_{ij} > r_e\end{cases} \tag{7}$$

where r_e is the search radius or called interaction radius, r_{ij} is the distance between the target particle i and surrounding particles j.

In the simulation, the parameter values of every target particle are determined by the surrounding particles. However, it is time consuming to calculate every particle interaction in the simulation, if the effect of every particle in the domain was considered simultaneously for a single target particle. To address and reduce the computation time, a search radius r_e is applied and the effect of the surrounding particles beyond the defined radius is not included in the computation. Constraining the search radius, $r_{e,}$ may cause reduced accuracy in the simulation results. Therefore, a proper value has to be selected for balancing the time constraints and simulation accuracy. In this paper, r_e is chosen as $4.0DL$ (DL is the diameter of numerical particle size), which has been shown to be an optimum value in obtaining accurate numerical results (Chambon et al. 2011, Vescovi et al. 2016).

when the particle relationships are converted through kernel function, the gradient terms and Laplacian terms in the governing equations are discretized as: (Koshizuka and Oka 1996), Fu and Jin 2013, Xu and Jin 2016).

The gradient model:

$$\left\langle \nabla \Phi \right\rangle_i = \frac{D_m}{n_0} \sum_{j \neq i} \frac{\Phi_j - \Phi_i}{r_{ij}^2} \boldsymbol{r_{ij}}\, w\left(r_{ij}, r_e\right) \tag{8}$$

The Laplacian model:

$$\left\langle \nabla^2 \Phi \right\rangle_i = \frac{2D_m}{\lambda n_0} \sum_{j \neq i} \left(\Phi_j - \Phi_i\right) w\left(r_{ij}, r_e\right) \tag{9}$$

in which Φ is a scalar, r_{ij} is equal to $|\boldsymbol{r_j}-\boldsymbol{r_i}|$, D_m is a number for space of dimension, n_0 is initial particle number density or average particle number density.

The value λ is defined as:

$$\lambda = \frac{\int_V r^2 w\left(r, r_e\right) \mathrm{d}V}{\int_V w\left(r, r_e\right) \mathrm{d}V} \tag{10}$$

In this study, all simulations are in a 2D coordinate system, so D_m is equal to 2. The initial value of the particle number density n_0 is determined at the initial time following:

$$\left\langle n \right\rangle_i = \sum_{j \neq i} w\left(r_{ij}, r_e\right) \tag{11}$$

The equation of state proposed by Batchelor et al. (1967) and Monaghan et al. (1994) is modified for MPS and applied in this study (Fu and Jin 2013, Xu and Jin 2016) to obtain the pressure field. In this study, the weakly compressible semi-implicit method (WC-MPS) is applied, unlike normal MPS method, it is assumed that the fluid has very small

compressibility (less than 1%) to model incompressible fluid. The equation of state is expressed as:

$$p_i^{k+1} = \frac{\rho c_0^2}{\gamma}\left[\left(\frac{\langle n\rangle_i^*}{n_0}\right)-1\right]^{\gamma} \tag{12}$$

where γ is equal to 7, and c_0 is the sound speed. Based on Mach number <0.1, the density change is smaller than 1% while $c_0 = 10U_{max}$ (U_{max} is the maximum velocity in numerical simulation), therefore, the artificial speed of sound is used instead of the real sound speed in MPS (Dalrymple and Rogers 1981). In order to obtain a condition of stability, the maximum time step has to satisfy CFL Courant-Friedrichs-Lewy (1967) condition:

$$\Delta t < \frac{CDL}{c_0} \tag{13}$$

In which $0 < C < 1$ is Courant number (Shakibaeinia and Jin 2011). In this paper, the Courant number is equal to 0.25 for every case.

2.2. Boundary condition

In this study, two types of boundary condition including solid boundary condition and free surface boundary condition are considered (Fu and Jin 2013, Ikari and Gotoh 2016, Xu and Jin 2016). The boundary particles are identified by the free surface condition to define the changing granular domain. The free surface condition is defined (Koshizuka et al. 1998):

$$\langle n \rangle_i^* < \beta n_0 \tag{14}$$

where the asterisk * represents an intermediate value, and n_0 is initial or average particle density, β is a constant which is usually taken from 0.8 to 0.99. The pressure is assigned to be zero, and shear stress will be imposed on the free surface.

In MPS, the solid boundary is treated as a combination of wall and ghost particles. Figure 2 illustrates the boundary conditions and particle distribution. The black particles in figure 2 represent the wall particles and several layers of ghost particles distributed below the wall particles. The interaction radius, r_e brings surrounding particles in the circle through the support of the kernel function. Without the help of ghost particles, the particle number density will be insufficient for the target particle near the solid boundary. In other words, ghost particles ensure that there are enough particles located in the searching radius.

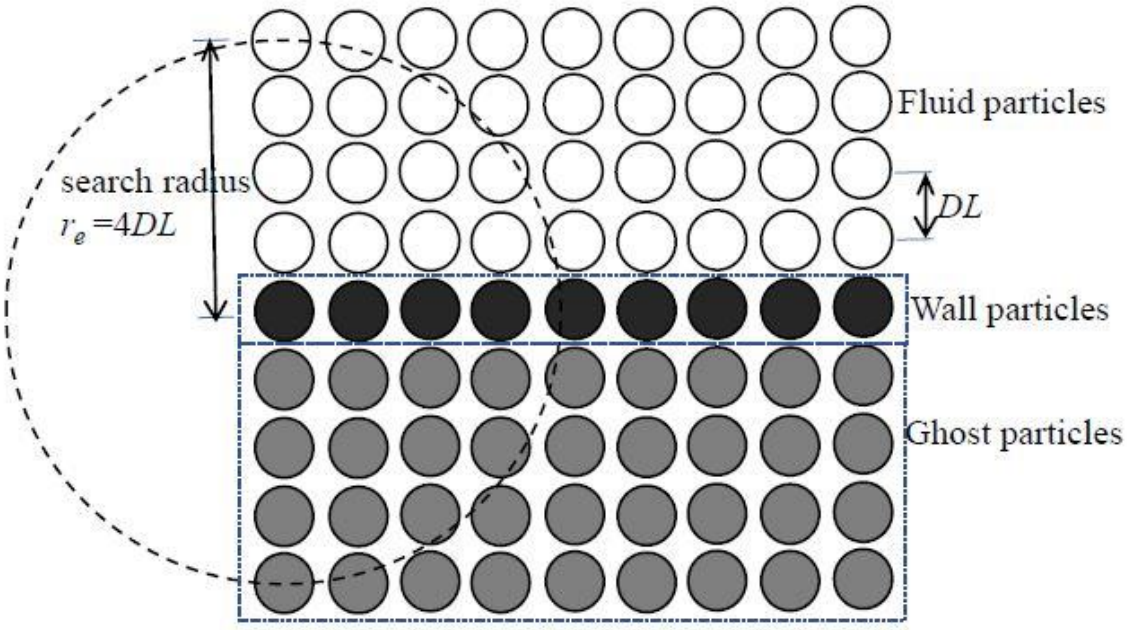

Figure 2 Solid boundary condition and particle types

In this study, the searching radius r_e=4.0DL has been successfully applied in simulating granular flow (Xu and Jin 2016). so, the r_e=4.0DL is chosen in this study. Because r_e=4.0DL, there are four layers of ghost particles beyond wall particles. The solid boundary is considered as a no-slip boundary, so the velocities of wall and ghost particles are equal to zero. For pressure and shear stress, the ghost particles have the same value as wall particles.

2.3. Rheology model

The rheology model, $\mu(I)$, can quantitatively predict flow properties of granular flow (Jop et al. 2006). The model is discussed and applied in numerical methods (Chambon et al 2011, Chauchat and Médale 2014, Vescovi and Luding 2016 and Xu and Jin 2016). The model is developed by assuming that the shear stress has a linear relation with the confining pressure as:

$$\tau = \mu p \tag{15}$$

where τ is shear stress, p is pressure and μ is friction factor. μ is locally dependent on the inertial number I, and the following equation is proposed by Cruz et al. (2005) to calculate the value of μ:

$$\mu(I) = \mu_s + \frac{\mu_2 - \mu_s}{\frac{I_0}{I} + 1} \tag{16}$$

where I_0 is a constant, μ_2 and μ_s is minimum and maximum coefficient of friction factor. respectively (Xu and Jin 2016). Theoretically, the flow regime is determined as quasi-static regime when the friction factor is smaller than the minimum friction factor, μ_s. When the friction factor begins to increase, the flow regime will transition from a quasi-static regime to the dense regime or even to the gaseous regime. In figure 3, it shows the fiction factor change against inertial number I. The minimum friction factor with minimum inertial energy corresponds to the quasi static regime. Once the inertial energy increases with increase of fiction factor, the flow regime is in the dense regime. Then, the very high

inertial number loses contact of granular particles, so, the flow regime is entering gas regime.

The equation of inertial number *I* is written as:

$$I = \frac{|\varepsilon| d}{\left(\frac{p}{\rho_s}\right)^{0.5}} \quad \text{with } \rho_s = \frac{\rho}{\phi} \tag{17}$$

where $|\varepsilon|=(0.5\varepsilon_{ij}\varepsilon_{ij})^{0.5}$ is second invariant of strain rate tensor and $\varepsilon_{ij} = \frac{\partial u_i}{\partial x_j} + \frac{\partial u_j}{\partial x_i}$ is the strain rate tensor, *d*, the diameter of granular material grain, the volume fraction ϕ, and ρ_s is actual density of granular material.

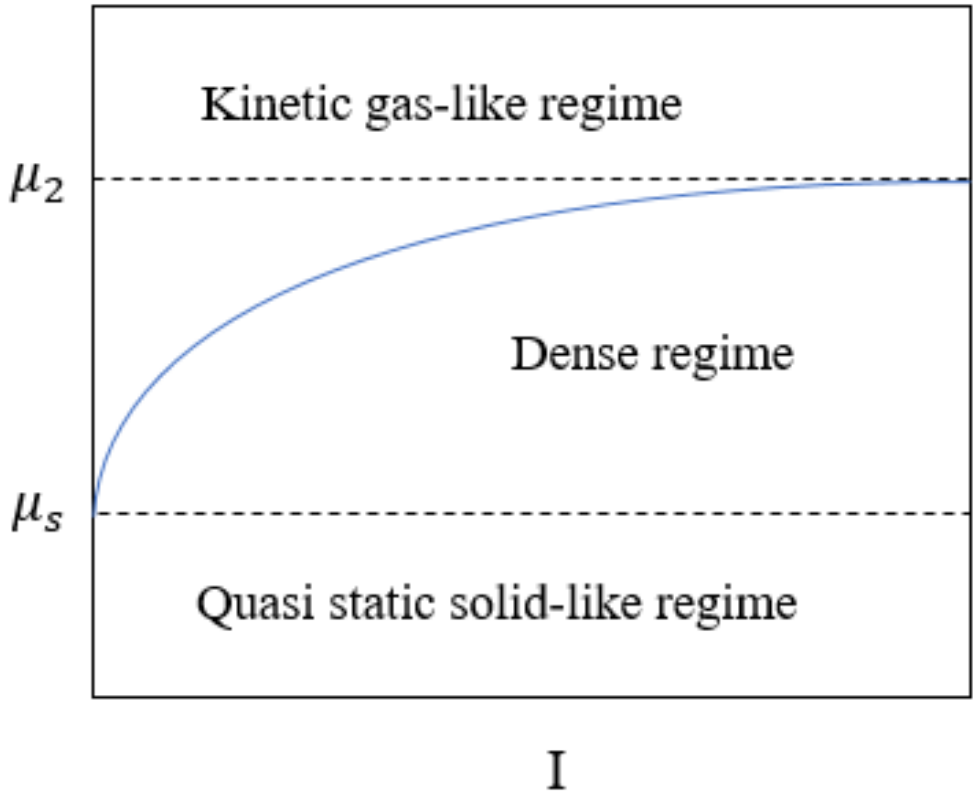

Figure 3 Friction factor against inertial number

Extending the constitutive law to a 2D or even 3D problem, the following equation is proposed by Jop et al (2006):

$$\tau_{ij} = \eta \varepsilon_{ij} \text{ with } \eta = \frac{\mu(I)p}{|\varepsilon|} \tag{18}$$

in which η is the effective viscosity, and τ_{ij} is the deviatoric stress tensor. This rheology model introduces a yield criterion (Jop et al. 2006) given as:

$$|\boldsymbol{\tau}| > \mu_s p \tag{19}$$

where $|\boldsymbol{\tau}|=(0.5\,\tau_{ij}\,\tau_{ij})^{0.5}$. The granular material only flows while Eq. (19) is satisfied.

However, a very small $|\varepsilon|$ will lead to an infinitely large value of η, which could be beyond the capacity of the computing in the simulations. In order to solve the problem, one method is to use a very large value of viscosity to constrain the value of η. This approach is also described and applied by Chambon et al. (2011):

$$\begin{cases} \tau_{ij} = \eta_t \varepsilon_{ij} & if \quad \dfrac{\mu_s p}{|\varepsilon|} > \eta_t \\ \tau_{ij} = \eta \varepsilon_{ij} & if \quad \dfrac{\mu_s p}{|\varepsilon|} < \eta_t \end{cases} \tag{20}$$

where η_t is the controlled viscosity, η_t =500 is proved to be effective in this study.

In this study, the constitutive parameters of granular material (glass beads) applied in numerical method include: μ_s=tan(20.90°) in Eq. (16), μ_2=tan(32.76°) in Eq.(16), diameter of granular material d=2.0 mm in Eq. (17), I_0=0.279 in Eq.(16). Other parameters will be introduced in each specific case.

CHAPTER THREE: Numerical simulations

Three different scenarios are applied to numerically validate the robustness of the coupled rheology model to the MPS method in simulating the transient deformational dynamics of granular flow conditions. The simulated results are compared to the analytical solutions

based on the pressure distribution, shear stress friction factor, surface, run-out distance and velocity of the flow characteristics.

The first scenario focused on the characteristics of the granular flow on a sloped channel. Pressure, shear stress, and velocity of the granular flow is compared between the analytical solution to the numerical simulations in order to validate the capability of the coupled model to reproduce the flow field from the sloped channel. The equation of the analytical velocity, derived from Bagnold's profile, will be used to validate the velocity extracted from the simulation based on the assumption of the steady flow on the inclined bed where shear stress balances the longitudinal component and pressure balances the vertical component. From above assumption, the analytical friction factor can be determined as the slope of channel and is equal to the ratio of shear stress to pressure. Pressure and shear stress is difficult to obtain comprehensively through experimental measurement. Especially, the important parameter of shear stress in granular flow is almost impossible to measure inside granular flow. As a result, the analytical velocity, friction factor, pressure and shear stress will be compared with numerical result.

In the second scenario, the coupled model is tested against the flow dynamics of a granular column collapse at different time steps. The column collapse is an important and ideal scenario to test and validate the coupled model because of the co-existence of flowing conditions such as the flowing region and the quasi-static regions that occurs simultaneously. The velocity, pressure and the shear stress distribution in the flowing region from the column collapse is compared to the coupled model. Because shear stress

measurement in column collapse is difficult to obtain in experimental settings, the shear stress is simulated and compared to the experimental data. In the 2D column collapse scenario, the velocity, pressure, shear stress distribution, and the friction factor is presented to illustrate the interrelationship within the different flow regimes. Although the shear stress is not validated through experimental results, the distribution of the shear stress shows the changes occurring in the different regions of the granular material within the column collapse.

In the last scenario, experimental data from a dam break is compared to the coupled model. The dynamic nature and flow deformation of the dam break provides confirmation of the capability and flexibility of the coupled model in simulating the flow characteristics and the distribution of the shear stress. The dam breaking scenario results in dynamic deformation of the free surface, which contains both the flowing, transitional and quasi-static region. Because the transitional region is of interest in column collapse experiments, the rheology model and MPS method will represent the dynamic nature of the flow characteristics

3.1. Steady flow down a sloped channel

The application of the coupled model was applied to a 2D simulation sloped channel since a zone of steady uniform flow exists in such conditions. Analytical solutions for the

pressure, velocity, and shear stress can be calculated within the steady, uniform zone of the sloped channel (Chambon et al. 2011, Pouliquen 1999). Figure 6 illustrates the experimental setup. A 0.25 m×0.25 m container filled with sufficient numbers of 2mm glass beads is placed on the upslope of a 2.5 m length channel at an angle of 24.5°. An aperture of 0.036 m located on the bottom right side of the container allows the granular material to escape and flow down the sloped channel. The configuration of the setup for the simulation results in a Froude number equal to 0.5, which results in a uniform and steady flow zone downstream of the aperture, if the slope of the channel is between $\tan^{-1}(\mu_s)$ and $\tan^{-1}(\mu_2)$.

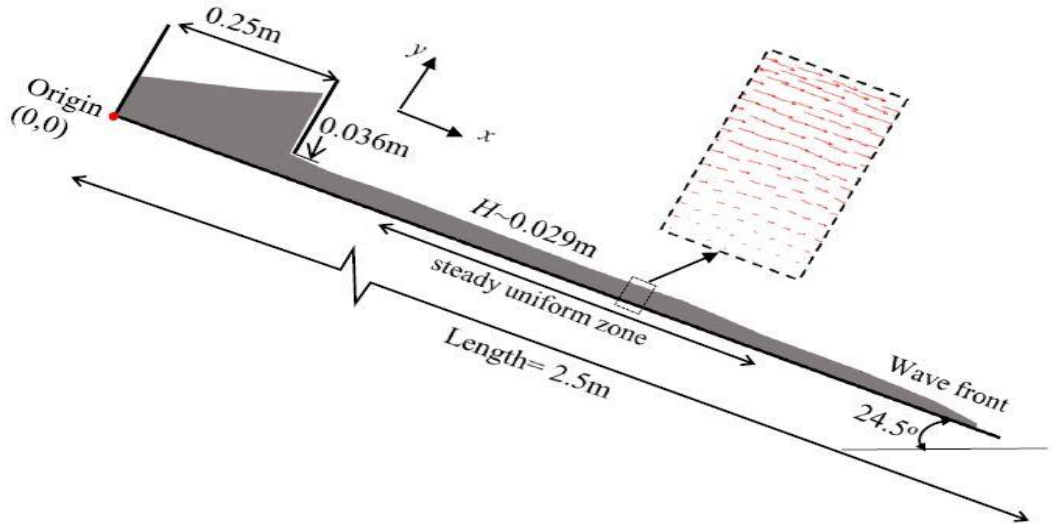

Figure 4 Geometric set up for granular material flow down sloped channel

$$\tau = \rho g(H-y)\sin\theta, \quad p = \rho g(H-y)\cos\theta, \quad \text{and} \quad \mu = \frac{\sin\theta}{\cos\theta} \tag{21}$$

where P is pressure, τ is shear stress, μ is friction factor, θ is angle of channel bed, H is depth of the flow perpendicular to the channel bed and y is target depth of the flow. By applying the definition of inertial number I, the velocity in the uniform zone yields a profile as (Chambon et al. 2011):

$$u = \frac{2}{3} I_\theta \sqrt{\phi \cos\theta} \left(\frac{H}{d}\right)^{3/2} \left(1 - \left(1 - \frac{y}{H}\right)^{3/2}\right) \sqrt{gd} \tag{22}$$

in which d is the diameter of the material grains. The value of inertial number I_θ is calculated by:

$$I_\theta = I_0 \frac{\tan\theta - \mu_s}{\mu_s + \Delta\mu - \tan\theta} \tag{23}$$

where $\Delta\mu = \mu_2 - \mu_s$ is equal to 0.26 and θ is the slope of the channel (Jop et al. 2006).

In the numerical simulation using the coupled model, a layer of granular material begins to flows along the channel bed from the container through the aperture. From figure 4, With time, the granular flow extends along the bed. Downstream of the aperture, a zone is observed with the velocity vectors parallel to the channel bed and show less change with time in the simulation. This layer is observed to have a constant total thickness H~0.0029m in the simulation, which is also observed in Chambon et al, (2011) and Pouliquen (1999). Another finding is that the length of uniform zone gradually extends with the wave front moving forward along the bed. In this uniform region, velocity profiles are extracted along

the thickness y at different locations. It should be noted that velocity profiles in the simulation are only extracted when a uniform zone is formed since the flow is not steady and uniform in the beginning of the simulations when the granular material start to flow out the container. Figure 5 shows the comparison between numerical and analytical velocity profiles in the uniform region at t=4 s and t=5 s, where the dimensionless velocity $U_d=(u^2+v^2)^{0.5}/(gH)^{0.5}$ is used. The solid line represents the analytical velocity profiles calculated by Eq. 22. In the figure 5, the dimensionless velocity profiles U_d of steady uniform zone are plotted against thickness y. Based on the velocity vector paralleled to slope in figure 6, the results show good agreement at the two time steps suggesting that the velocity perpendicular to the channel bed in the zone is very small. This also helpfully suggests a steady uniform region in the flow.

The numerical solution shows good agreement with the analytical solution by showing a linear velocity distribution for $y\leq$0.02 m (Figure 5). The linear velocity distribution in the linear velocity profile has been shown in previous studies (Pouliquen 1999). However, for y>0.02 m, there is a discrepancy between the numerical results and the analytical velocity profiles. This could be due to the boundary condition in the coupled method and a different regime occurring in the flow. The granular grains flow with a higher velocity compared to other grains resulting in the interaction between grains dominated by binary collision. Hence, the flow close to the free surface may be in the gaseous regime. However, in the simulation by using the coupled model, the flow is still modeled by using a continuum approach rather than by kinematic theory for the gaseous regime (Xu and Jin 2016). On the other hand, the free-surface part only occupies several particles or points in the simulation

by using the mesh-free method. Taking the particle distance DL=0.002m as an example, there are four particles for the free-surface part comparing 10 particles below the free surface. The assumption of analytical velocity is that the friction factor is a constant value, but the numerical friction factor is not constant under surface condition since the pressure is extremely low. The comparison shows that the coupled model is able to capture the velocity information in this steady uniform flow region with discrepancy observed on the free surface.

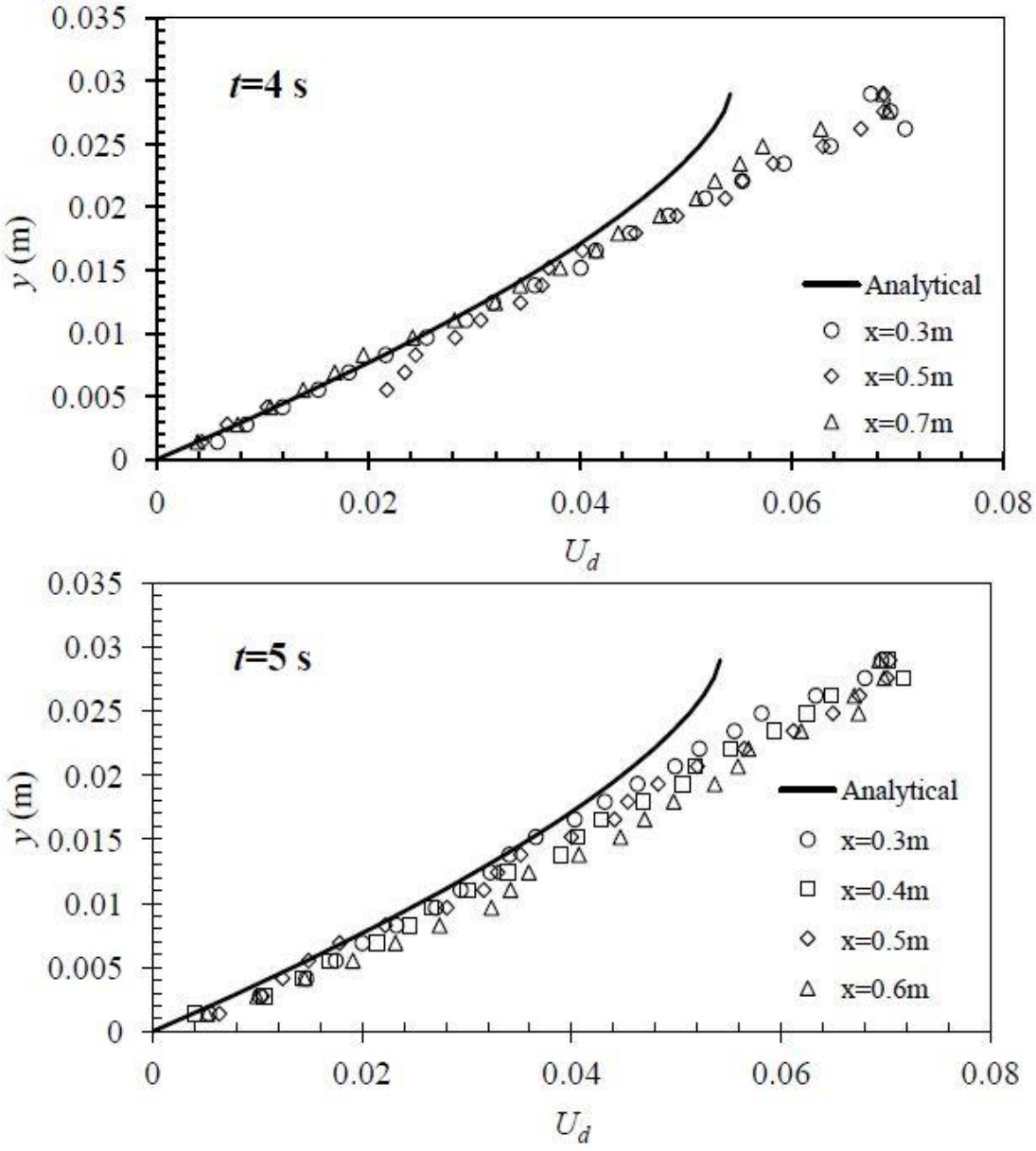

Figure 5 Velocity distribution along depth in a sloped channel

The friction factor is calculated and compared between numerical and analytical results. Figure 6 illustrates the numerical and analytical friction factors at two different time steps (t=4 s and t=5 s) along the flow depth y. In this uniform region, the friction μ remains constant. Based on Eqs. (16) and (17), the value of friction factor is related to the pressure and the numerical values are calculated by using the pressure field in the simulation. It shows that the numerical friction factors have good agreement with the analytical results below the free surface. There is a deviation to the constant friction on the free surface in Figure 6. The maximum fluctuation of friction factor is around $\pm$ 0.11.

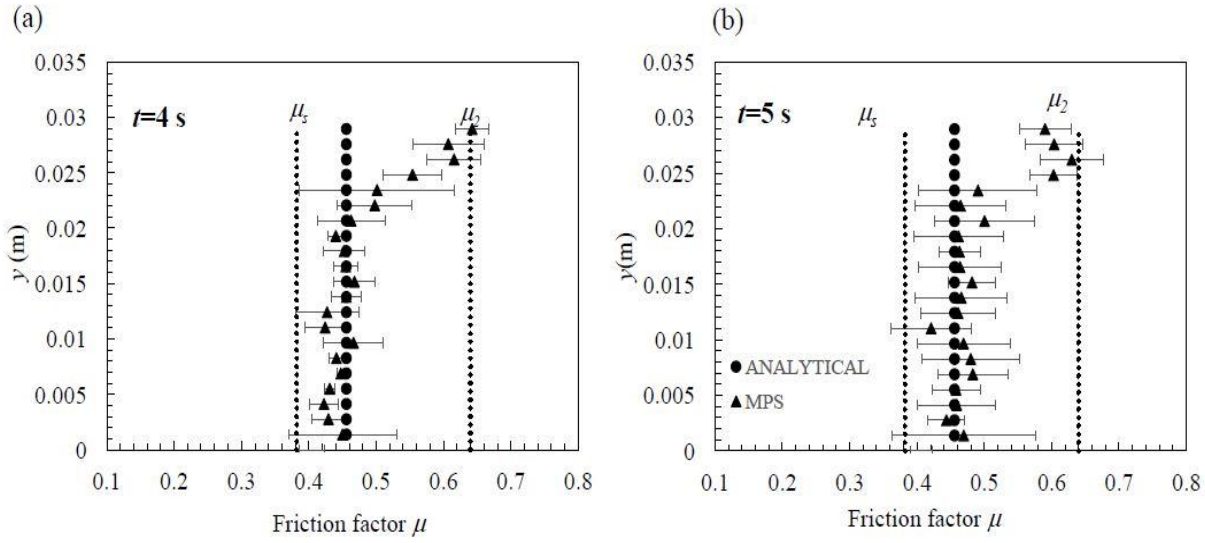

Figure 6 Distribution of friction factor along depth at (a) t=4s and (b) t=5s.

The distribution of numerical pressure and shear stress have been compared with the analytical results (Figure 7a,b). In this case, the analytical shear stress calculated by Eq. (18) is related to pressure multiplying a constant fiction factor μ=tan (24.5°). Therefore, the analytical shear stress is linearly distributed since pressure has linear distribution. However, fluctuations are observed in the numerical simulations of the pressure and shear stress. These deviations from the linear distribution could be by the assumption that the flow is weakly-compressible and using an equation of state to obtain the pressure field. Although fluctuations are observed, the numerical result can be explained by a linear trend line. The slopes of the fitted line for both the pressure and shear stress in the numerical results are similar to the analytical equation. Hence, the coupled model is able to capture characteristics of the pressure and shear stress in the uniform region for the flow down an inclined channel. Meanwhile, fluctuations in the numerical results are also found due to the assumptions in the model.

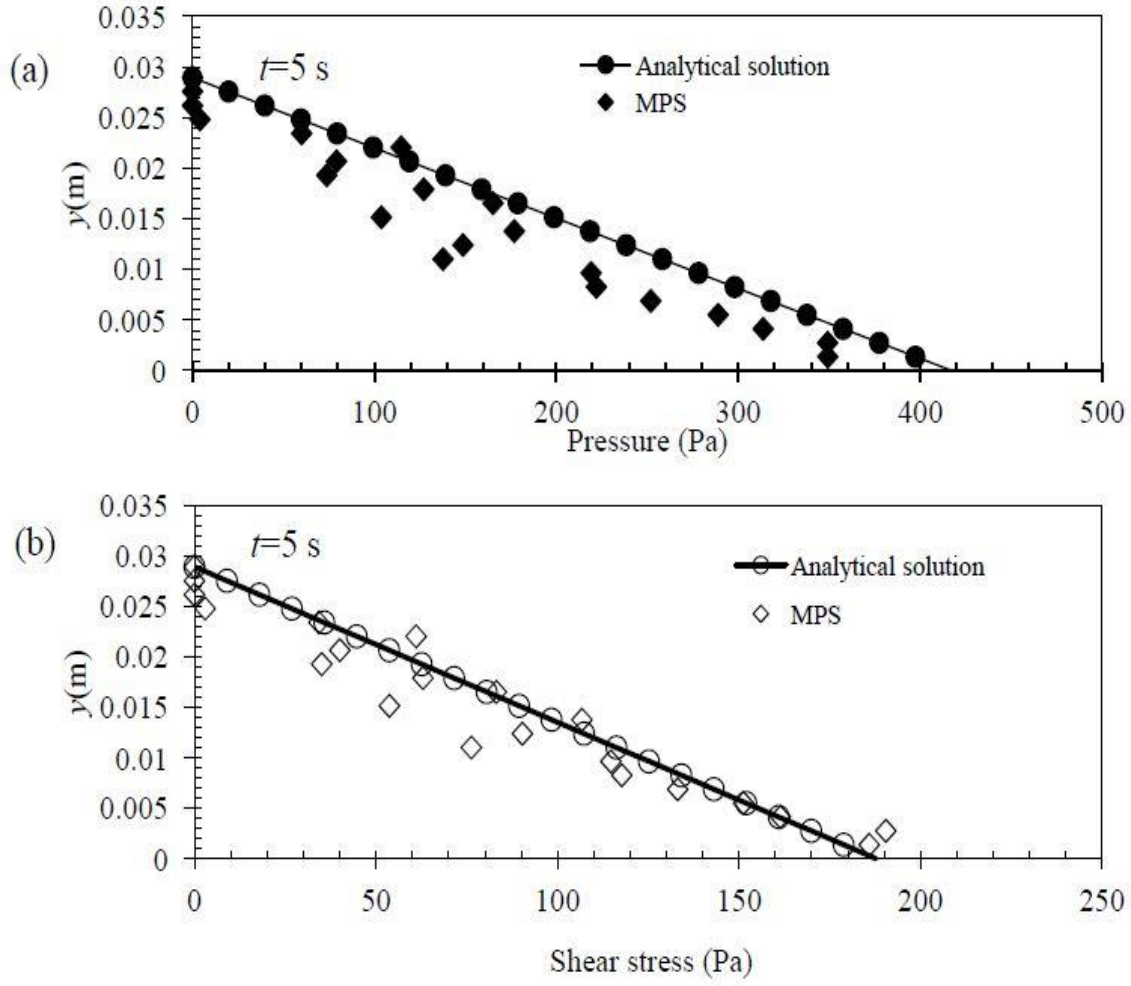

Figure 7 Pressure and shear stress distribution along depth at *t*=5s

3.2. 2D Granular Column collapse

In this section, granular flow is modeled as granular column collapse. Figure 8 illustrates the experimental setup of the granular column with an initial aspect ratio of $a = H/L = 1.25$. The granular material collapse and distributes outward onto a horizontal plate upon lifting of a gate by a constant force weight. The granular material column consists of glass beads with diameter of d = 2 mm. The bulk density of the glass beads is ρ=2500 kg/m^3. The velocity is measured from the side through applying PIV technique (Xu et al. 2017). A 2D numerical modeling is conducted by following the experimental configuration. There are a total number of 2945 particles with particle size DL = 0.0025 m in the simulation to represent the granular column.

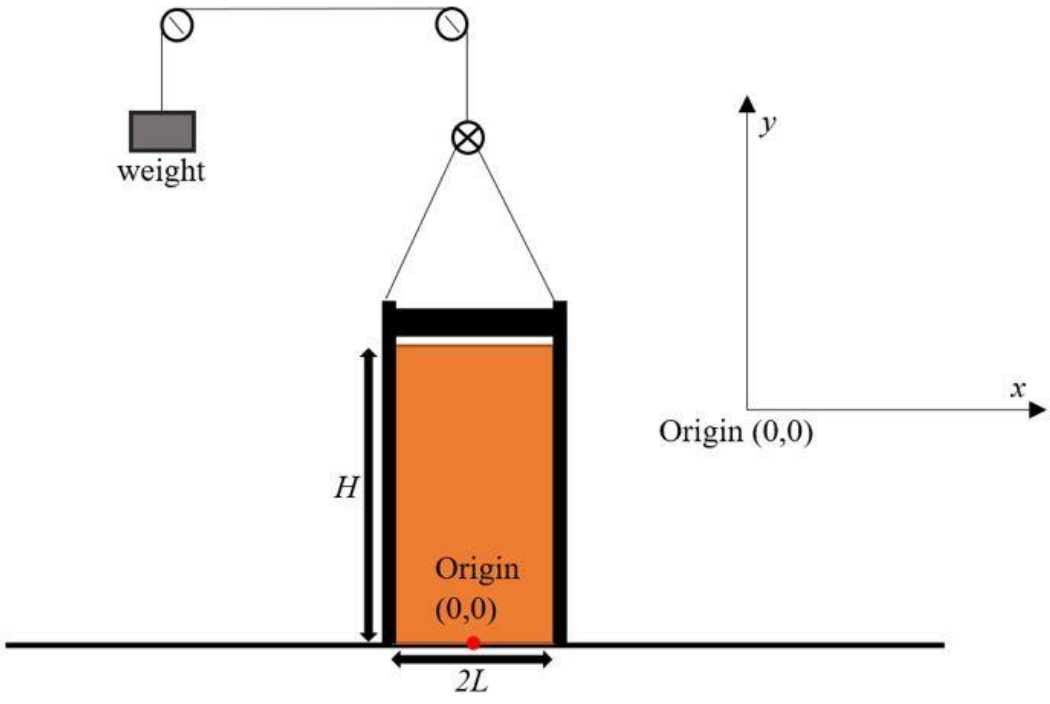

Figure 8 experimental set up of 2D column collapse

Velocity profiles from both the MPS simulation and experimental column along depth are plotted at different vertical sections (x = ± 0.01m, x = ± 0.02m, x = ±0.03m, x = ± 0.04m) with the origin of the coordinate in the center on the bottom of the column (Figure 10). Figures 9 and 10 shows the velocity distributions with $U=(u^2+v^2)^{0.5}$, respectively at t=0.129 s and 0.269 s. The velocity distribution from the numerical simulation agrees well with the experimental measurements at both time steps. The general trend of the velocity profile shows that it is small close to the bottom and then greatly increases to the free surface. For the sections close to the center such as x = ± 0.01m, a larger part of velocity profiles remains close to zero. Because the gate removal still affects the movement of granular material in the experimental data at t =0.129s, the numerical result slightly over predicts the velocity at beginning. At t =0.269 s, the effect of gate removal dissipated and, it appears that there is better agreement between the simulated results to the experimental data as compared to t=0.129s.

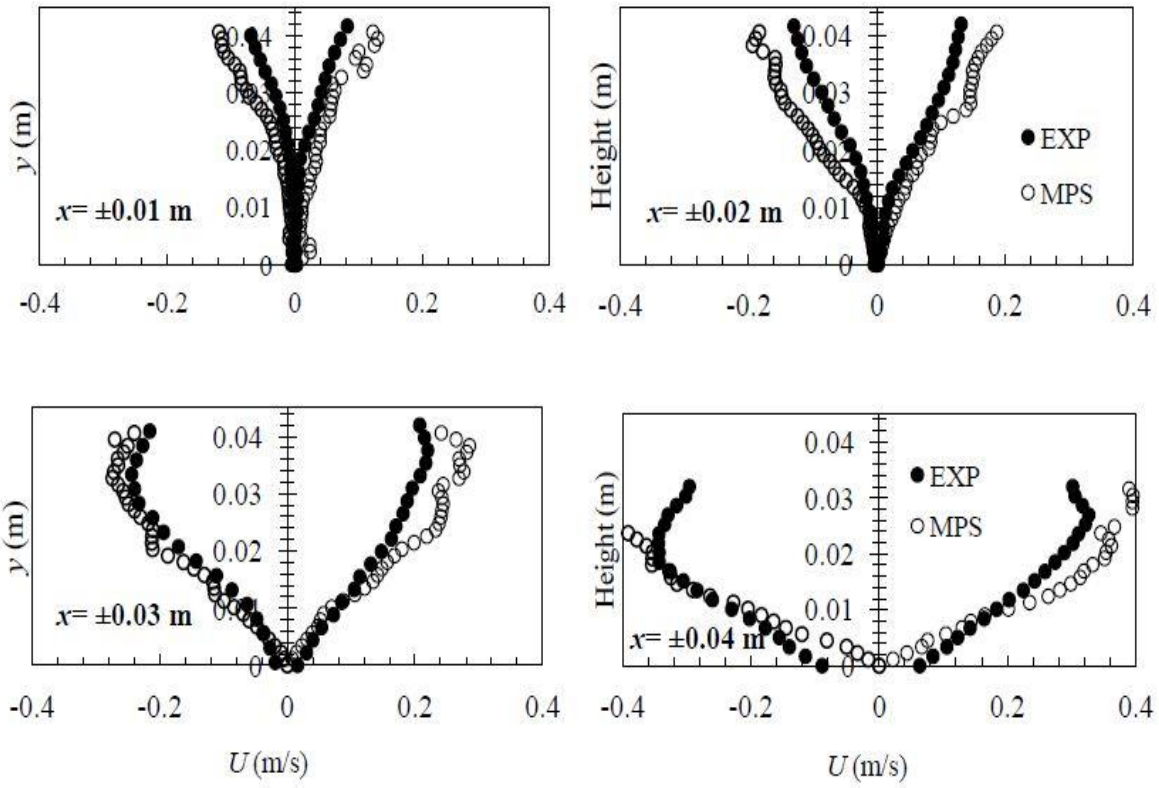

Figure 9 Velocity distribution along depth y at t=0.129 s

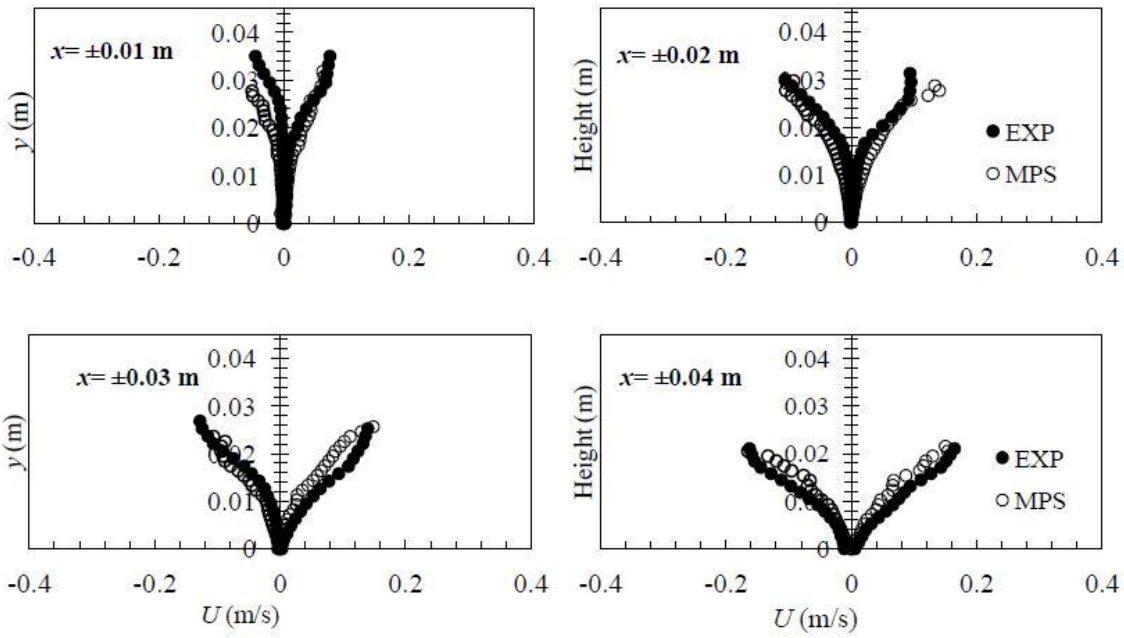

Figure 10 Velocity distribution along depth at t=0.269 s

Similar to the initial scenario, the comparison of pressure and shear stress distribution for the coupled model and analytical solutions shows that MPS method coupled with the $\mu(I)$ rheology model can reasonably capture pressure and shear stress in the granular flow. Figures 11 and 12 illustrate the distributions of pressure and shear stress along depth at two time steps obtained in the simulation. Different from the uniform steady flow in the previous case, the pressure and shear stress distributions in the granular column collapse show to be non-linear in the *y* direction. The pressure and shear stress display a larger-value distribution in the center of the column shown in the two figures. The numerical results for these distributions correspond to the granular column collapse while a thicker layer of material located at the center, making the pressure and shear stress larger. The collapse resulted in a very highly unsteady flow with deformation of the free surface, and therefore, the distributions of pressure and shear stress are non-linear.

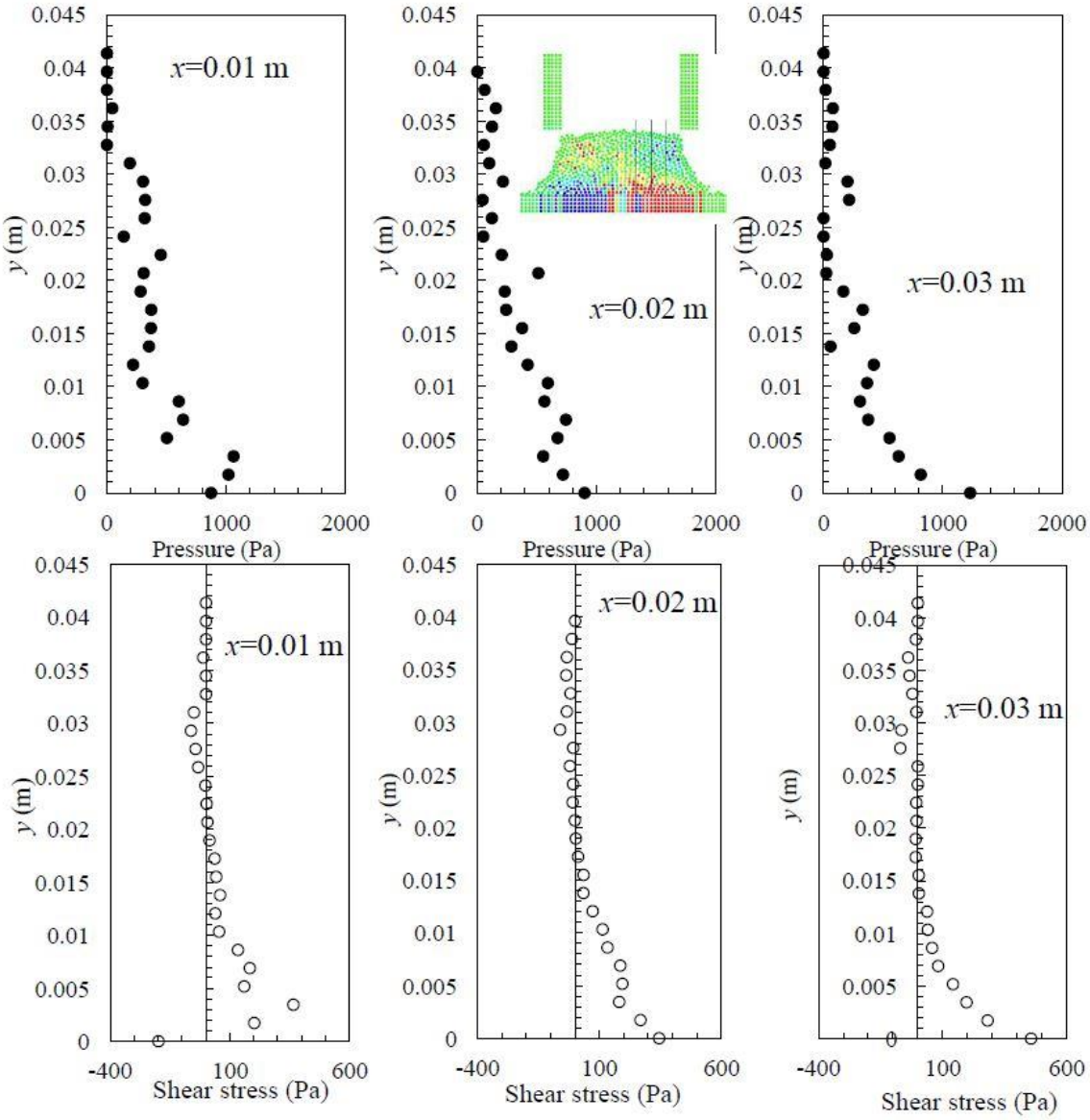

Figure 11 Numerical pressure and shear stress distribution along depth at t=0.129 s

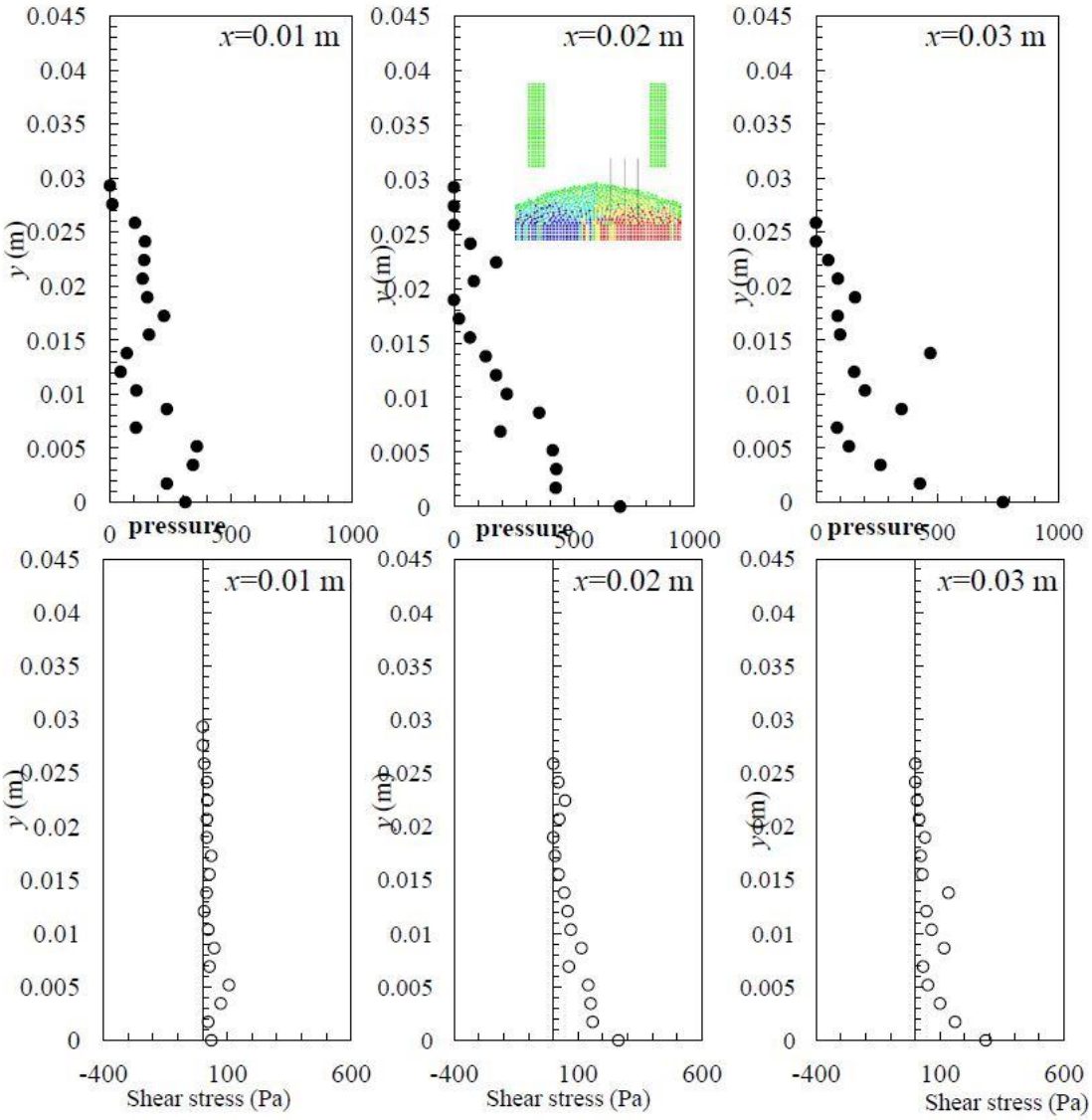

Figure 12 Numerical pressure and shear stress distribution along depth y at t =0.269 s

The inertial number in the simulation calculates the friction factor according to Eq. 17. At t=0.129 s, velocity and friction factor start to increase and the shear stress is minimal at value above y=0.02 m. Between y=0.01 m and y=0.02 m, very small velocity still exists. Below y=0.01 m, velocity is almost equal to zero and the shear stress tends to increase clearly. By looking at pressure distribution, the obvious increase of pressure occurs below y=0.01 m. At t=0.269 s, the high pressure and high shear stress corresponds to small friction factor. The zone with low pressure and low shear stress corresponds to high friction factor.

Figures 13 and 14 illustrates the distribution of friction factor in the simulation. The friction obtained in the simulation is in the range of μ_s and μ_2 indicating that the flow is in the dense regime for the granular column collapse. The friction factor in the figures is small and the increase of friction factor for y<0.02m is almost close to zero near the bottom of the section during the collapse, but it increases for y>0.02 m when it is close to the free surface. For y<0.02m, the friction factor is almost constant since this zone where has low inertial has very low friction factor. Based on figure 3, the zone with low inertial has small friction factor. This is different from the 1st scenario because the collapse occurs on a horizontal plate such that the surface grains are not strongly agitated to make them display gaseous feature. For example, if the flow is produced on a sloped plate, the slope may accelerate the flow especially for the grains on the free surface. With a higher slope angle, greater agitation of the granular material will likely occur resulting in the grains to behave similar to the gaseous regime.

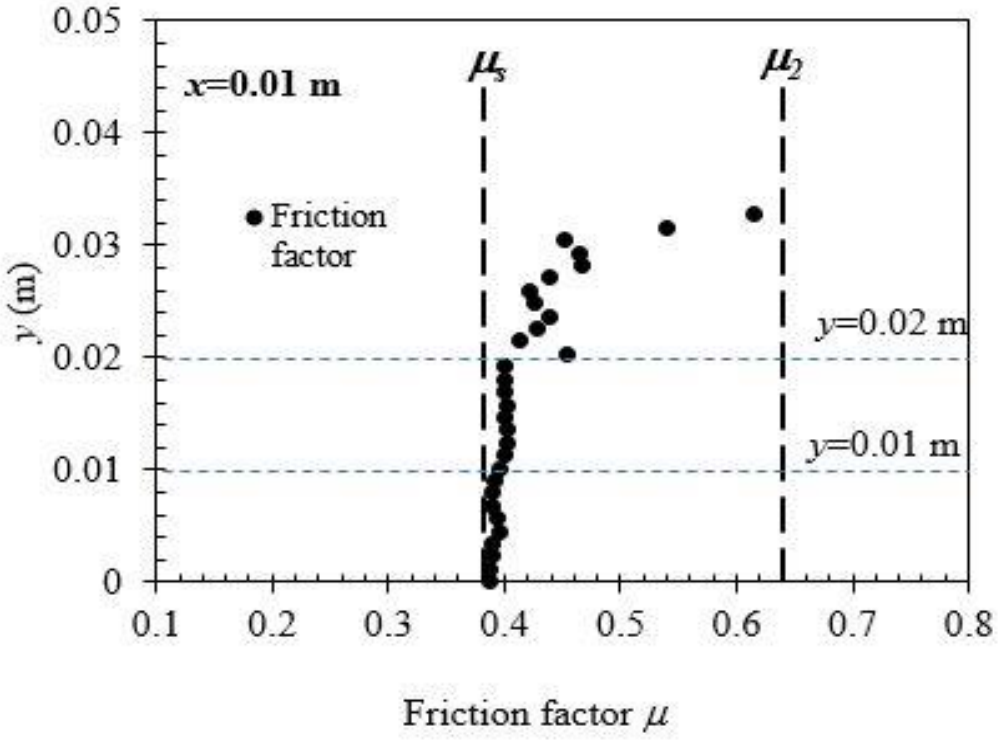

Figure 13 Distribution of friction factor along depth at t=0.129 s

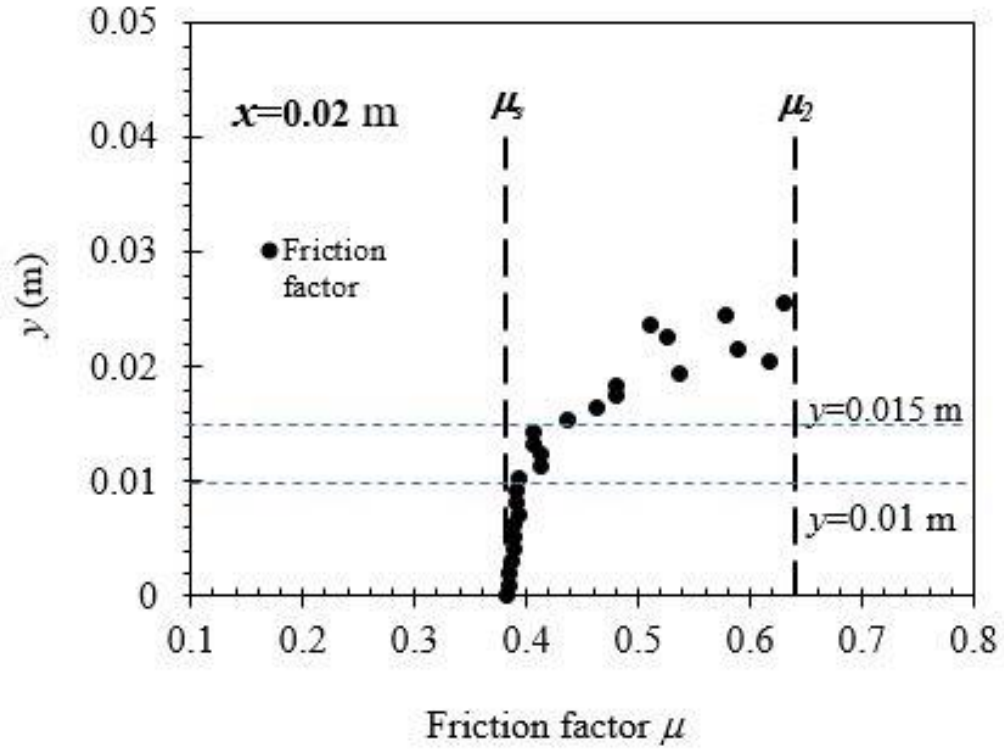

Figure 14 Distribution of friction factor along depth at t=0.269 s

3.3 Granular dam-break

The dam breaking flow is a widely used case scenario to test the mesh-free particle method. The coupled rheology model, with the MPS method, is compared to experimental data completed by Xu et al. (2016). Figure 15 illustrates the numerical domain with a rectangular column of granular ceramsite (diameter d=5 mm) of initial column height, H=0.18m and width L=0.1m placed on a plate. The pressure measurement is conducted by using a layer of tactile sensor on the bottom of the granular column to record pressure change along the bottom of the plate. The bulk density of the granular material is 2200 kg/m^3. The granular dam break is initiated by quickly lifting the baffle which allows the granular material to be instantly released. In the simulation, the particle distance is DL=0.002m with a total number of 8294 particles in the column. The artificial sound of speed c_0=10 m/s is 10 times the maximum velocity in the problem. The parameters for the rheology model are the same as in the previous two scenarios since the static angle of ceramite is 22±2° similar to glass beads.

Figure 16 illustrates the free surface profiles with comparison to the experimental measurements by Xu et al. (2016). The coupled model captures the free surface in the dam break, showing a good agreement at different time steps in the flow process.

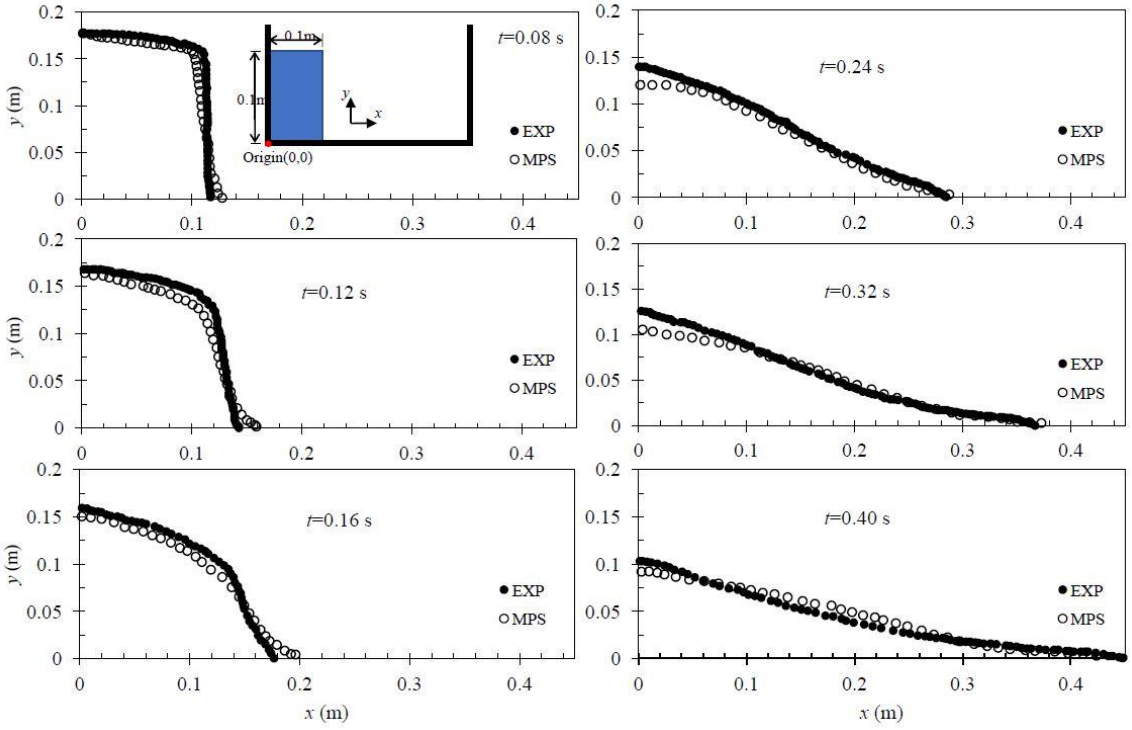

Figure 15 Surface comparisons between numerical results and experimental data of granular dam break

Previous work has shown that the initial aspect ratio $a=H_0/L_0$ where H_0 is initial height of granular column and L_0 is the initial width of granular column plays a very important role in granular column collapse (Lajeunesse et al. 2004, Lube et al. 2005). For $H_0/L_0 < 0.7$, the granular material results in truncated deposit. For $0.7 < H_0/L_0 < 3$, a conical shape deposit of granular pile can be formed. For $H_0/L_0 \geq 3$, a "Mexican hat" deposit appears. In this case, a=1.8, a smooth and stretched deposit is observed on the plate in the simulation. The horizontal extension of the granular pile can be clearly observed at t=0.08 s, 0.12 s, 0.16 s, 0.24 s, 0.32 s, and 0.40 s. Before t=0.16 s, the wave front in the simulation propagates slightly faster than experimental observation. However, after t=0.24 s, the runout distance matches the experimental results as well.

Figure 16 shows the pressure comparison between the numerical and experimental results at three different time steps at $t=1.5\tau_c$, $t=2\tau_c$, and $t=3\tau_c$ *with* $\tau_c=(H/g)^{0.5}$. As shown in the figure, the pressure is not linearly distributed in both the experiment and simulation. In the experimental measurements, the pressure at each position x is the averaged value over the 20 sensels in the transverse direction, producing a smooth pressure distribution. The pressure from the simulation shows fluctuation since they are instantaneous pressures determined at every time step Δt=0.00005s. However, this fluctuation is around the experimental pressure distribution which is measured longer than the numerical time step. This fluctuation in the numerical results may also come from the weakly-compressible treatment for the flow although fluctuation for velocity and pressure exists in granular

flows as suggested (Xu et al. 2016). Here, we highlight the pressure distribution trend is reflected by the numerical model.

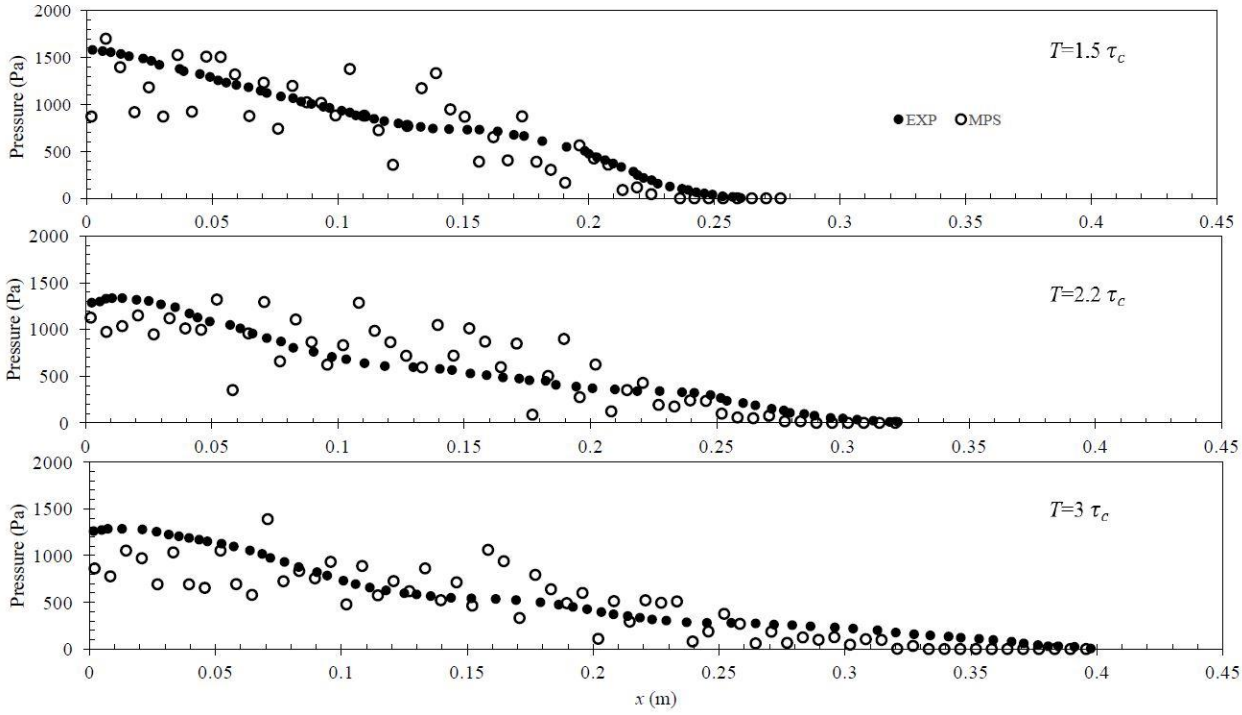

Figure 16 Pressure comparisons between numerical results and experimental data along bottom

The velocity contour in the simulation is compared with the experimental observation in Figure 17. Column failure starts from initial state (t=0) while the potential energy of the column transfers to kinetic energy. From t=0.6τ_c, three zones of velocity magnitude are observed in both numerical and experimental velocity contours, including a high-velocity zone close to the free surface marked in the red color, a quasi-static zone located in the left corner, and a zone with intermediate velocity between the two zones. From t=0 to 1.2τ_c, it is clear that the thickness of the high-velocity zone increases while intermediate-velocity zone decreases. The area occupied by the quasi-static zone shows minimal change in the flow regime. Between t=1.2τ_c to 3.5τ_c, both the high-velocity and intermediate-velocity zones gradually disappear due to energy dissipation while the quasi-static zone is extended along the plane. Good agreement between the simulation and experiment measurements in the evolution the shape of the collapse is attained.

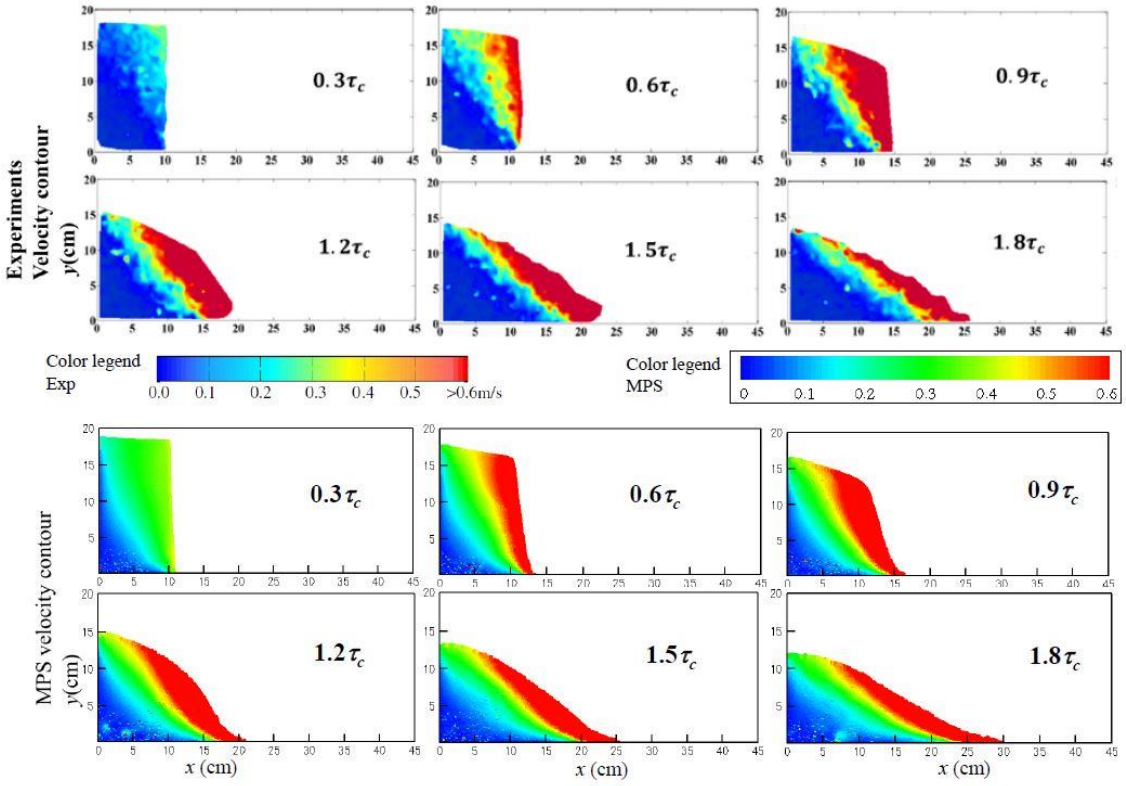

Figure 17 Numerical and experimental (Xu et al 2016) velocity contour comparison

Figure 18 shows the pressure and shear stress distributions at three different time steps and at different vertical sections. It is obvious that the pressure increases with the depth in the flow. The pressures at x=6 cm at t=1.2 τ_c and 1.8 τ_c, the pressure distribution is pseudo-linear; however, fluctuations still occur because this is the quasi-static region where the movement of particles are very small. In the flowing region, the pressure no longer appears to be linear such as at x=0.14 m at t=1.8 τ_c. In terms of shear stress, it shows a similar shape and trend as pressure. Based on the rheology model, the shear stress is pressure-dependent, resulting in a similar distribution to the pressure in the flow.

The friction factor obtained in the simulation at x=0.06 m is shown in Figure 19. The calculated friction factor is between μ_s and μ_2, indicating the flow is in the dense regime. A vertical red line is drawn at x=6cm on velocity contour. It is clear that for y<0.05 m, the friction is very small but friction factor is still larger than μ_s where the velocity field in both the experiment and simulation shows to be small as a quasi-static region. For y>0.05 m, the particles move in considerable velocity, increasing the friction factor but still smaller than μ_2, thus, the flow still in the dense regime rather than the gaseous regime. This characteristic also exists in other locations and time steps

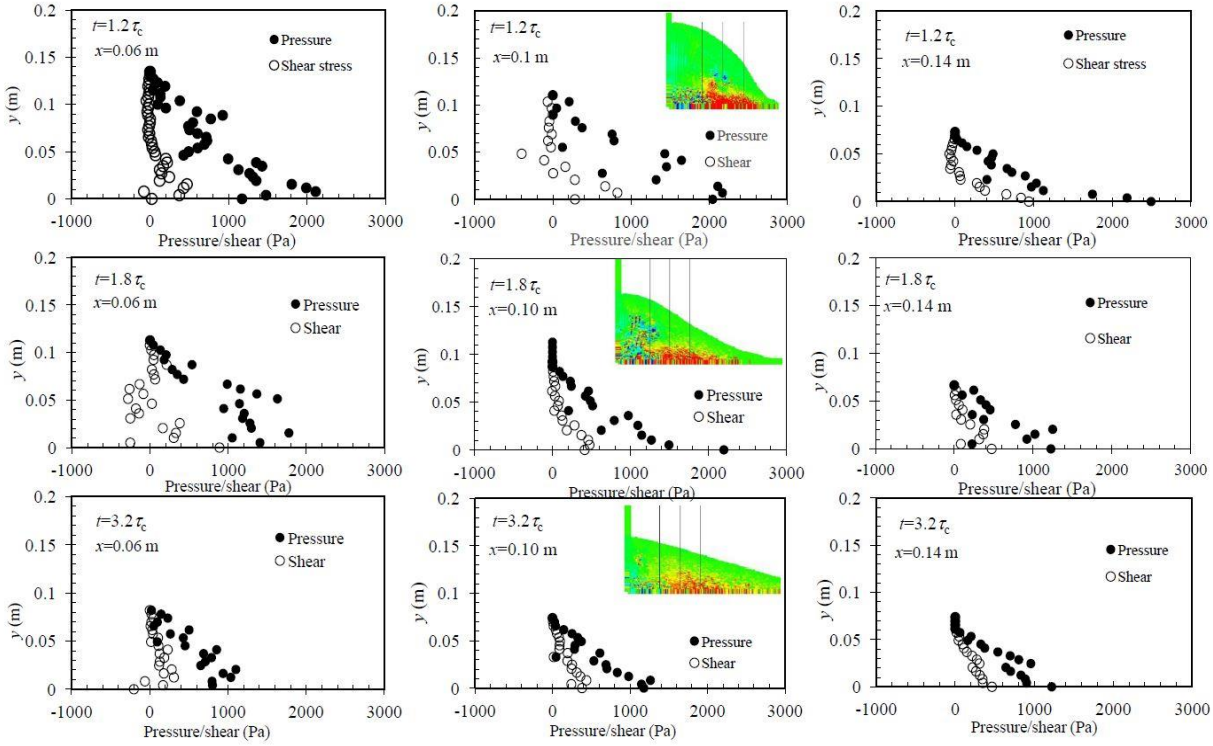

Figure 18 MPS results of distribution of pressure and shear stress along depth *y*

.

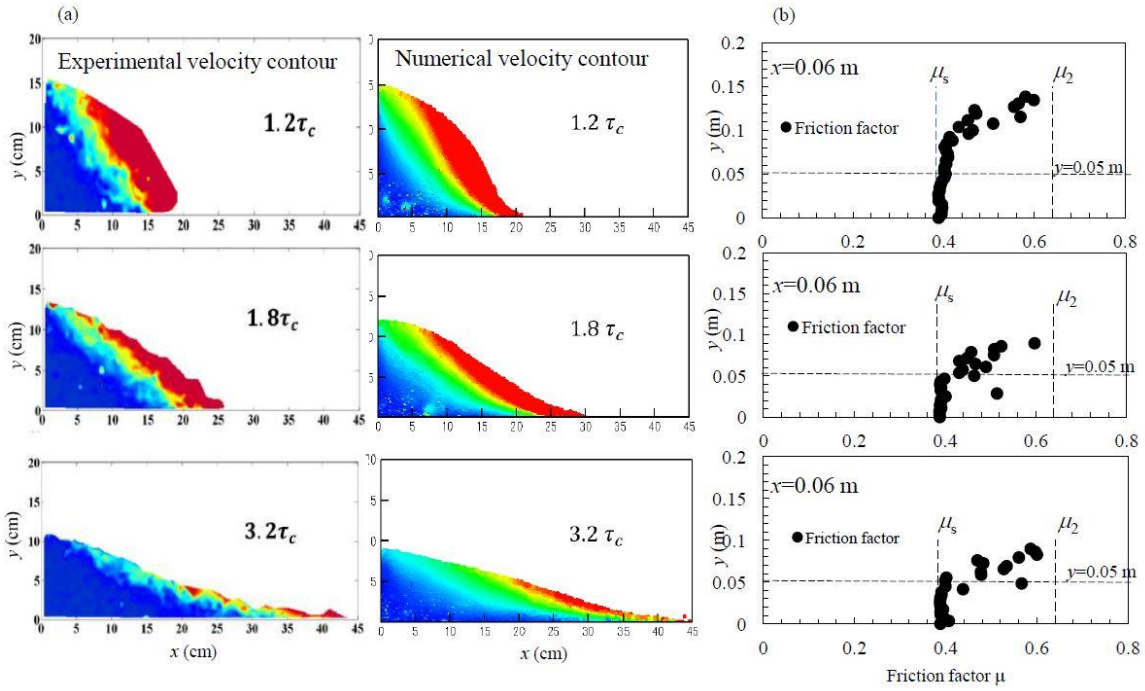

Figure 19 (a) Numerical and experimental velocity contour and (b) numerical distribution of friction factor.

CHAPTER FOUR: Summary

4.1 conclusion

In this study, the idea of coupled $\mu(I)$ rheology model from Xu, T., & Jin, Y. (2016) has been applied to three scenarios. The successful application of model extends the applicability of this coupled model. The MPS method coupled with $\mu(I)$ rheology model is applied to model three different scenarios, which includes flow down an inclined plate, granular column collapse, and granular dam break, to validate the flexibility of the coupled model in simulating deformation flow conditions under various conditions. The numerical results are compared with analytical solutions and experimental measurements. The velocity and pressure distributions as well the friction factor is analyzed and discussed for each case.

For the flow down an inclined plate, there is a steady uniform flow region. The coupled model is used to capture the dynamics in this region and the numerical results are compared with the analytical solutions for the flow region. The model indeed reproduces the uniform flow zone where all velocity vectors parallel to the sloping plate and a constant thickness of the flow (H=0.029 m) is maintained to a considerable distance. The linear velocity distribution below the free surface is captured by the model, which shows good agreement with the analytical solutions. In this flow, the presence of a considerable slope angle 24.5° accelerates the flow especially for the granular grains on the free surface, making them behave like gaseous feature. This feature for the free surface particles is further confirmed by the calculated friction factor, μ, which is very small and larger than maximum coefficient of friction factor μ_s, for y<0.02 m but is greater than minimum coefficient of

friction factor μ_2 close to the free surface. Therefore, the discrepancies for the velocity distribution on the free surface are observed between the numerical and analytical results since these gaseous free grains are modeled by treating it as a continuum in the dense regime in the numerical method. Although the numerical results display fluctuation for the pressure and shear stress distributions, the analytical solutions are accurately represented by the coupled model.

A 2D granular column collapse is then modeled by the coupled model with comparison to experimental measurements for the velocity distribution. The simulated velocity profiles have a good agreement with the measured velocity distribution in the collapse. In this case, the collapse occurs on a horizontal plate such that the free surface grains could not be strongly agitated. The calculated friction factor shows that the flow is in the dense regime where $\mu_s<\mu<\mu_2$. Since the granular column collapse is a highly unsteady flow with large deformation of free surface, the pressure and shear stress are not linearly distributed. As non-linear distribution, the pressure and shear stress increase with the flow depth.

The mentioned two granular flows modeled by the coupled model showed the flexibility and robustness of the model to represent the velocity distribution by comparing results with analytical and experimental measurements. A granular dam break is further modeled to highlights that the coupled model is able of calculating the pressure in the flow by comparing with experimental measurements for the pressure distribution. Firstly, the surface profiles are plotted and the numerical results show good agreement with the measurements. By calculating the friction factor, the flow is in the dense regime. The non-

linear pressure distribution is reproduced by the coupled model. Although the modeled pressure has some fluctuations, it agrees well with the experimental measurements in the comparison. The shear stress in the simulation in the flow has similar distribution to the pressure.

Through the simulation of three different granular flows with different configurations, the coupled model as the MPS with the $\mu(I)$ rheology model are shown to be able to capture many dynamics for the flows in the dense regime, such as velocity, pressure, free surface, and shear stress. However, it should be noted that when or a flow includes multiple regimes such as the intermediate dense regime and gaseous regime, the coupled model has difficulty to reflect the dynamics beyond the dense regime. This study focuses on the flow modeling in the dense regime and achieve a good result. But the limitation of this coupled model is that the accurate transitions between behaviors is not represented and the coupled model may only reproduce the local correlations. So, to develop a generous model to capture more flow dynamics such as crossing regimes is our future work.

4.2 possible approach of future work

In above study, applying the rheology model coupled with MPS shows its capability in different scenarios. All comparison of pressure, velocity and surface have achieved acceptable results. But, few results still need to be discussed or verified. As mentioned in the study, to measure experimental pressure and shear stress inside granular flow is very difficult. So, the numerical pressure and shear stress calculated in MPS is only validated through analytical solution under specific condition. If the pressure and shear stress inside

granular flow could be obtained accurately, more discussion of pressure and shear stress could be displayed. Except the difficult measurement of pressure and shear stress in experiment, the fluctuation of pressure and shear stress is interesting approach. Discussed in Hostler, S. R., & Brennen, C. E. (2005), pressure fluctuation is normal phenomenon in granular propagation, because of the heterogeneity and nonlinearity in granular system. The fluctuation in numerical result corresponds to experimental result. However, the extent of fluctuation is an interesting approach as well.

Acknowledgement

This research was supported in part by the Natural Sciences and Engineering Research Council of Canada (109585-2012). We thank Dr. Y.C. Tai from National Cheng Kung University to provide experimental data for comparison.

Reference

Batchelor, G. K. (1967). An introduction to fluid dynamics, Cambridge Univ. Press, Cambridge, UK.

Capart, H., Hung, C., & Stark, C. P. (2015). Depth-integrated equations for entraining granular flows in narrow channels. *Journal of Fluid Mechanics, 765*. doi:10.1017/jfm.2014.713

Chambon, G., Bouvarel, R., Laigle, D., & Naaim, M. (2011). Numerical simulations of granular free-surface flows using smoothed particle hydrodynamics. *Journal of Non-Newtonian Fluid Mechanics,166*(12-13), 698-712. doi:10.1016/j.jnnfm.2011.03.007

Chauchat, J. and Médale, M., (2014). A three-dimensional numerical model for dense granular flows based on the μ (I) rheology. *Journal of Computational Physics, 256*, pp.696-712.

Courant, R., Friedrichs, K., and Lewy, H. (1967). "On the partial difference equations of mathematical physics." IBM J. Res. Dev., 11(2), 215–234(English translation of the 1928 German original).10.1147/rd.112.0215

Cruz, F. D., Emam, S., Prochnow, M., Roux, J., & Chevoir, F. (2005). Rheophysics of dense granular materials: Discrete simulation of plane shear flows. Physical Review E, 72(2). doi:10.1103/physreve.72.021309

Dalrymple, R., & Rogers, B. (2006). Numerical modeling of water waves with the SPH method. *Coastal Engineering, 53*(2-3), 141-147. doi:10.1016/j.coastaleng.2005.10.004

Forterre, Y., & Pouliquen, O. (2008). Flows of Dense Granular Media. Annual Review of Fluid Mechanics, 40(1), 1-24. doi:10.1146/annurev.fluid.40.111406.10214

Fu, L., & Jin, Y. (2015). Investigation of non-deformable and deformable landslides using meshfree method. *Ocean Engineering, 109*, 192-206. doi:10.1016/j.oceaneng.2015.08.051

Fu, L., & Jin, Y. (2013). A mesh-free method boundary condition technique in open channel flow simulation. *Journal of Hydraulic Research, 51*(2), 174-185. doi:10.1080/00221686.2012.745455

Hirt, C., & Nichols, B. (1981). Volume of fluid (VOF) method for the dynamics of free boundaries. *Journal of Computational Physics, 39*(1), 201-225. doi:10.1016/0021-9991(81)90145-5

Ikari, H., & Gotoh, H. (2016). SPH-based simulation of granular collapse on an inclined bed. *Mechanics Research Communications, 73*, 12-18. doi:10.1016/j.mechrescom.2016.01.014

Jin, Y., Guo, K., Tai, Y., & Lu, C. (2016). Laboratory and numerical study of the flow field of subaqueous block sliding on a slope. *Ocean Engineering, 124*, 371-383. doi:10.1016/j.oceaneng.2016.07.067

Jop, P., Forterre, Y., & Pouliquen, O. (2006). A constitutive law for dense granular flows. *Nature, 441*(7094), 727-730. doi:10.1038/nature04801

Koshizuka, S. and Oka, Y., (1996). Moving-particle semi-implicit method for fragmentation of incompressible fluid. *Nuclear science and engineering, 123*(3), pp.421-434.

Koshizuka, S., Nobe, A., & Oka, Y. (1998). Numerical analysis of breaking waves using the moving particle semi-implicit method. *International Journal for Numerical Methods in Fluids, 26*(7), 751-769. doi:10.1002/(sici)1097-0363(19980415)26:7<751::aid-fld671>3.3.co;2-3

Lagrée, P., Staron, L., & Popinet, S. (2011). The granular column collapse as a continuum: validity of a two-dimensional Navier–Stokes model with a μ(I)-rheology. *Journal of Fluid Mechanics, 686*, 378-408. doi:10.1017/jfm.2011.335

Lajeunesse, E., Mangeney-Castelnau, A., & Vilotte, J. P. (2004). Spreading of a granular mass on a horizontal plane. *Physics of Fluids, 16*(7), 2371-2381. doi:10.1063/1.1736611.

Lube, G., Huppert, H. E., Sparks, R. S., & Freundt, A. (2005). Collapses of two-dimensional granular columns. Physical Review E, 72(4). doi:10.1103/physreve.72.041301

MiDi, G. (2004). On dense granular flows. *The European Physical Journal E, 14*(4), 341-365. doi:10.1140/epje/i2003-10153-0

Monaghan, J. J. (1994). "Simulating free surface flows with SPH." J. Comput. Phys., 110(2), 399–406.10.1006/jcph.1994.1034

Pouliquen, O. (1999). Scaling laws in granular flows down rough inclined planes. *Physics of Fluids, 11*(3), 542–548. doi:10.1063/1.869928.

Shakibaeinia, A., & Jin, Y. (2011). MPS-Based Mesh-Free Particle Method for Modeling Open-Channel Flows. *Journal of Hydraulic Engineering, 137*(11), 1375-1384. doi:10.1061/(asce)hy.1943-7900.0000394.

Shakibaeinia, A., and Jin, Y. C. (2010). "A weakly compressible MPS method for simulation open-boundary free-surface flow." Int. J. Numer. Methods Fluids, 63(10), 1208–1232.10.1002/fld.2132

Vescovi, D., & Luding, S. (2016). Merging fluid and solid granular behavior. *Soft Matter,12*(41), 8616-8628. doi:10.1039/c6sm01444e

Xu, T., & Jin, Y. (2016). Modeling free-surface flows of granular column collapses using a mesh-free method. *Powder Technology, 291*, 20-34. doi:10.1016/j.powtec.2015.12.005.

Xu, X., Sun, Q., Jin, F., & Chen, Y. (2016). Measurements of velocity and pressure of a collapsing granular pile. *Powder Technology,303*, 147-155. doi:10.1016/j.powtec.2016.09.036

Xu,T., Jin,Y. Tai, Y. & Lu, C. (2017). Numerical analysis of velocity and shear stress distributions in granular column collapses by a mesh-free method. *Journal of Non-Newtonian Fluid Mechanics,* 247, 146-164. Doi: m10.1016/j.jnnfm.2017.07.003

Sela, N., & Goldhirsch, I. (1998). Hydrodynamic equations for rapid flows of smooth inelastic spheres, to Burnett order. *Journal of Fluid Mechanics, 361*, 41-74. doi:10.1017/s0022112098008660

Garzó, V., & Dufty, J. W. (1999). Dense fluid transport for inelastic hard spheres. *Physical Review E, 59*(5), 5895-5911. doi:10.1103/physreve.59.5895

Liu,N. (2015) Hongshiyan landslide dam danger removal and coordinated management Front, Eng.Manag.1, 308-317. 2015.

Andreotti, B., 2007. A mean-field model for the rheology and the dynamical phase transitions in the flow of granular matter. *EPL* (*Europhysics Letters*),*79*(3), p.34001.

Brodu, N., Richard, P. and Delannay, R., 2013. Shallow granular flows down flat frictional channels: Steady flows and longitudinal vortices. *Physical Review E*, *87*(2), p.022202.

de Gennes, P.G., (1999). Granular matter: a tentative view. *Reviews of modern physics, 71*(2), p.S374

Jaeger, H.M., Nagel, S.R. and Behringer, R.P., (1996). Granular solids, liquids, and gases. *Reviews of Modern Physics*, *68*(4), p.1259

Takahashi, T.(2014). *Debris flow: mechanics, prediction and countermeasures*. CRC Press.